

## Grown-in defects limiting the bulk lifetime of p-type float-zone silicon wafers

N. E. Grant, F. E. Rougieux, D. Macdonald, J. Bullock, and Y. Wan

Citation: *Journal of Applied Physics* **117**, 055711 (2015); doi: 10.1063/1.4907804

View online: <http://dx.doi.org/10.1063/1.4907804>

View Table of Contents: <http://scitation.aip.org/content/aip/journal/jap/117/5?ver=pdfcov>

Published by the [AIP Publishing](#)

---

### Articles you may be interested in

[The effect of oxide precipitates on minority carrier lifetime in p-type silicon](#)

*J. Appl. Phys.* **110**, 053713 (2011); 10.1063/1.3632067

[Reduction of grown-in defects by vacancy-assisted oxygen precipitation in high density dynamic random access memory](#)

*Appl. Phys. Lett.* **83**, 4863 (2003); 10.1063/1.1632536

[Trapping of gold by nanocavities induced by H + or He ++ implantation in float zone and Czochralski grown silicon wafers](#)

*J. Appl. Phys.* **90**, 2806 (2001); 10.1063/1.1394917

[Effects of oxygen-related defects on the leakage current of silicon p/n junctions](#)

*J. Appl. Phys.* **84**, 3175 (1998); 10.1063/1.368470

[External gettering by aluminum–silicon alloying observed from carrier recombination at dislocations in float zone silicon wafers](#)

*Appl. Phys. Lett.* **70**, 2744 (1997); 10.1063/1.119009

---

Frustrated by old technology?      Is your AFM dead and can't be repaired?      Sick of bad customer support?



**It is time to upgrade your AFM**  
Minimum \$20,000 trade-in discount for purchases before August 31st

**Asylum Research is today's technology leader in AFM**

[dropmyoldAFM@oxinst.com](mailto:dropmyoldAFM@oxinst.com)



The Business of Science®

## Grown-in defects limiting the bulk lifetime of *p*-type float-zone silicon wafers

N. E. Grant,<sup>a)</sup> F. E. Rougieux, D. Macdonald, J. Bullock, and Y. Wan

*Research School of Engineering, College of Engineering and Computer Science, Australian National University, Canberra, ACT 2601, Australia*

(Received 16 November 2014; accepted 28 January 2015; published online 6 February 2015)

We investigate a recombination active grown-in defect limiting the bulk lifetime ( $\tau_{bulk}$ ) of high quality float-zone (FZ) *p*-type silicon wafers. After annealing the samples at temperatures between 80 °C and 400 °C,  $\tau_{bulk}$  was found to increase from  $\sim 500 \mu\text{s}$  to  $\sim 1.5 \text{ ms}$ . By isochronal annealing the *p*-type samples between 80 °C and 400 °C for 30 min, the annihilation energy ( $E_{ann}$ ) of the defect was determined to be  $0.3 < E_{ann} < 0.7 \text{ eV}$ . When the annihilated samples were phosphorus gettered at 880 °C or subject to 0.2 sun illumination for 24 h,  $\tau_{bulk}$  was found to degrade. However, when the samples were subsequently annealed at temperatures between 250 and 400 °C, the defect could be re-annihilated. The experimental results suggest that the defect limiting the lifetime in the *p*-type FZ silicon is not related to fast diffusing metallic impurities but rather to a lattice-impurity or an impurity-impurity metastable defect. © 2015 AIP Publishing LLC.

[<http://dx.doi.org/10.1063/1.4907804>]

### I. INTRODUCTION

High purity and high lifetime monocrystalline silicon is becoming ever more important for very high efficiency solar cells. Understanding and mitigating the recombination activity of embedded impurities/defects in such material has been, and remains, an important topic.

In *p*-type boron-doped Czochralski (Cz) grown-silicon, the dominant recombination active centre is the boron-oxygen defect. While the composition of the boron-oxygen defect is not well understood, there have been processes developed to mitigate its recombination activity, such as hydrogenation,<sup>1–3</sup> gallium doping,<sup>4</sup> and oxygen-lean growth methods such as magnetic Cz (MCz) and Floating-zone (FZ).<sup>5</sup> While FZ silicon is more expensive to produce than Cz and mc-Si, it comes with the advantage of lower oxygen concentrations and thus, lower concentrations of other oxygen-related recombination-active defects such as oxygen precipitates and stacking faults.<sup>6–8</sup>

Considering the potential of *p*-type float-zone silicon for high efficiency silicon solar cells, it is critical to determine whether such material also contains impurities, grown-in defects, and metastable defects, which can reduce the bulk lifetime ( $\tau_{bulk}$ ). This is also important given that FZ silicon is often used as a control material when analysing bulk silicon defects or for surface passivation studies, where the recombination characteristics of the control sample is often assumed to be due to the surfaces and not the bulk. Evidently, these assumptions are not always true, and FZ silicon may contain substantial concentrations of extrinsic and intrinsic defects, which may limit/change  $\tau_{bulk}$  before, during or after various processing steps.<sup>9–11</sup>

In this paper, we examine a defect limiting the lifetime of FZ *p*-type silicon in the as-grown state. We examine the deactivation kinetics of the defect by annealing samples at

temperatures between 80 °C and 400 °C for 30 min. The annihilation energy of the defect is determined and its capture cross section ratio estimated by a Shockley-Read-Hall (SRH) analysis from the injection dependent lifetime. Finally, we examine the activation of the defect through light induced degradation (LID) experiments and high temperature phosphorus gettering and demonstrate that the defect is bistable.

### II. BACKGROUND

The incorporation of grown-in defects involving vacancies, self-interstitials, dislocations, and stacking faults during the growth of FZ ingots can be influenced by growth rates, temperature gradients, and cooling rates.<sup>9,10,12</sup> Previous studies have shown that slow growth rates ( $< 4 \text{ mm/min}$ ) can increase the formation of swirl defects which are highly recombination active. On the other hand, high growth rates can freeze-in silicon vacancies, which are recombination active when paired with an impurity atom such as phosphorus, boron, oxygen, hydrogen, or nitrogen.<sup>11,13–16</sup> Slow cooling rates ( $\ll 100 \text{ °C/min}$ ) help to maintain a defect lean high lifetime material by suppressing the concentration of frozen-in defects.<sup>9,10</sup> On the contrary, fast cooling rates ( $> 100 \text{ °C/min}$ ) can induce the formation of thermally activated defects, which if present in large quantities, can be recombination active and reduce the lifetime below the millisecond range.<sup>9,10</sup> Therefore, depending on each manufacturer's growth conditions, FZ silicon wafers of the same doping and type may result in completely different lifetimes and behaviour under various thermal processes.

Incorporation of light impurities such as oxygen, carbon, and hydrogen during the formation of FZ silicon ingots is expected to be low. Aside from oxygen,<sup>17</sup> the recombination activity of these impurities is not well understood, and their impact on the lifetime, even at low concentrations ( $< 1 \times 10^{16} \text{ cm}^{-3}$ ), is not known.<sup>18,19</sup> Thus, it cannot be assumed that impurities unintentionally incorporated into

<sup>a)</sup>Author to whom correspondence should be addressed. Electronic mail: [nicholas.grant@anu.edu.au](mailto:nicholas.grant@anu.edu.au)

the FZ ingot will not degrade the minority carrier lifetime to some extent, especially if they interact with other intrinsic defects within the silicon crystal. Recently, Rougieux *et al.* have shown that nitrogen-related defects (possibly vacancy-nitrogen pairs) could be responsible for a significant reduction in  $\tau_{bulk}$  observed in *n*-type FZ silicon, where  $[N] = \sim 5 \times 10^{14} \text{ cm}^{-3}$ .<sup>20</sup> This result is significant, as nitrogen is commonly used during the growth of FZ ingots, and in some cases, intentionally incorporated to improve the mechanical strength of the crystal, i.e., to avoid the formation of voids.<sup>21</sup> On the contrary, Cizsek *et al.* have found that in most cases N doping had little to no impact on  $\tau_{bulk}$  (where  $\tau_{bulk} \approx 4 \text{ ms}$ ).<sup>9,15</sup> In one case, however, N doping was found to increase  $\tau_{bulk}$  by eliminating swirl type defects. A similar result was achieved by hydrogen doping; however, significant reductions in  $\tau_{bulk}$  were observed for H doped silicon crystals.<sup>9</sup>

Oxygen contaminated *p*-type FZ silicon has been shown to significantly reduce  $\tau_{bulk}$  after illumination for several hours. Such degradation has been attributed to the formation of boron-oxygen (BO) complexes.<sup>22</sup> While this commonly occurs in Cz silicon, as-grown FZ silicon has been shown not to degrade under illumination,<sup>23</sup> even though oxygen concentrations on the order of  $\sim 10^{15} \text{ cm}^{-3}$  are typically present in this material.<sup>19</sup> Recently, Savin *et al.* have shown that copper related defects can also become activated under illumination and significantly degrade the lifetime in both *n*- and *p*-type FZ silicon.<sup>24</sup> It was shown that Cu concentrations of  $\sim 10^{13} \text{ cm}^{-3}$  had no impact on the lifetime when  $\tau_{bulk} = 200 \text{ } \mu\text{s}$ ; however, for much higher lifetime FZ silicon, Cu of  $\sim 10^{13} \text{ cm}^{-3}$  reduced  $\tau_{bulk}$  from 8 ms to 2 ms after 30 min of illumination. This demonstrates that high lifetime silicon is more sensitive to low concentrations of impurities, and thus one must be conscious of other impurities/defects which could also degrade  $\tau_{bulk}$  under illumination or during thermal processing, even in FZ silicon.

### III. EXPERIMENTAL METHODS

The samples under investigation were boron doped FZ silicon wafers from two different ingots with resistivities of 0.8  $\Omega \text{ cm}$  and 1.1  $\Omega \text{ cm}$ . The thickness of the wafers was 300  $\mu\text{m}$  and 500  $\mu\text{m}$ , respectively, and their diameter was 100 mm. To examine the impact of annealing temperature on the bulk lifetime, minority carrier lifetime measurements were performed using a room temperature surface passivation technique.<sup>25</sup> By this technique, silicon wafers were immersed into a container filled with 150 ml of 20 wt. % hydrofluoric acid (HF) and centred over an inductive coil for transient photoconductance (PC) measurements (using a WCT-120 system from Sinton Instruments).<sup>26</sup> To activate the surface passivation, the wafers were subsequently illuminated at 0.2 suns for 1 min using a halogen lamp, the light source was switched off, and a transient measurement was immediately performed. To achieve a very low  $S$  of less than 1 cm/s on *p*-type silicon,<sup>27</sup> the wafers were chemically treated prior to immersing the wafers into the HF solution. The chemical treatment involved two steps: (1) the wafers were etched in 25 wt. % tetramethylammonium hydroxide

(TMAH) at 80–90 °C for 10 min (removing about 5  $\mu\text{m}$  of silicon per side) and (2) the wafers were subsequently cleaned in RCA 1 at  $\sim 70$  °C for an additional 10 min. This chemical treatment ensures that the silicon surface is defect and contaminant lean.

Samples for phosphorus gettering were RCA cleaned and placed into a quartz boat, which was subsequently loaded into a quartz tube furnace. The samples were then subject to a phosphorus diffusion at 880 °C for 30 min, resulting in a sheet resistance of 23  $\Omega/\text{sq}$ . The samples were cooled to 600 °C and remained at this temperature for 15 h in  $\text{N}_2$  to further getter any fast-diffusing metal impurities within the silicon samples.<sup>28</sup> After removing the samples from the furnace, they were TMAH etched for 5 min at 80–90 °C to remove the phosphorus diffusion.

To investigate the possibility of light induced degradation during the HF measurements, minority carrier lifetime measurements were performed using a WCT-120 lifetime tester on samples with alternative passivation methods. To ensure that surface recombination did not significantly impact the lifetime measurements, the boron doped samples were passivated with a 20 nm atomic layer deposition (ALD)  $\text{Al}_2\text{O}_3$  film. Prior to the depositions, all samples received a damage etch in 25 wt. % TMAH at 80–90 °C for 10 min followed by a standard RCA clean. The  $\text{Al}_2\text{O}_3$  films were deposited at 200 °C using a Beneq TFS200 ALD system. Post deposition, the  $\text{Al}_2\text{O}_3$  films were annealed in forming gas at 400 °C for 30 min to activate the surface passivation.

## IV. RESULTS AND DISCUSSION

### A. Room temperature bulk lifetime measurements

Figure 1(a) plots the injection dependent bulk lifetime for FZ 0.8  $\Omega \text{ cm}$  *p*-type samples as measured by the HF passivation technique.<sup>25</sup> At low temperatures 20–130 °C, the defect remains activated, evident by the low lifetime and the typical SRH injection dependence. However, after subjecting the samples to a higher temperature anneal 150–200 °C, the lifetime at low injection ( $\Delta n < 1 \times 10^{15} \text{ cm}^{-3}$ ) increases and the shape of the curve becomes less injection dependent. When the samples are annealed at temperatures  $\geq 250$  °C, the lifetime saturates and becomes injection independent at low  $\Delta n$ , and thus indicates that the defect has been annihilated, as higher temperature annealing does not improve the lifetime further.

Figure 1(b) plots the bulk lifetime of FZ 0.8 (blue circles) and 1.1  $\Omega \text{ cm}$  (orange circles) *p*-type samples at  $\Delta n = 1 \times 10^{15} \text{ cm}^{-3}$  versus annealing temperature, for an annealing time of 30 min. The figure clearly demonstrates a substantial increase in  $\tau_{bulk}$  when annealing the samples between temperatures of 150–250 °C. From our measurements, it becomes clear that the maximum lifetime of each sample is not close to the predicted  $\tau_{intrinsic}$  value ( $\tau_{intrinsic} = 2.5 \text{ ms}$  and 4.2 ms for 0.8 and 1.1  $\Omega \text{ cm}$  *p*-type silicon, respectively<sup>29</sup>) and thus we attribute this additional bulk recombination to a second defect, which will be shown and discussed in Sec. IV D.2 The blue and brown solid lines of Figure 1(b) represent the best fit to the experimental data with an annihilation energy of 0.59 and 0.46 eV, respectively, and will also be discussed in Sec. IV B.

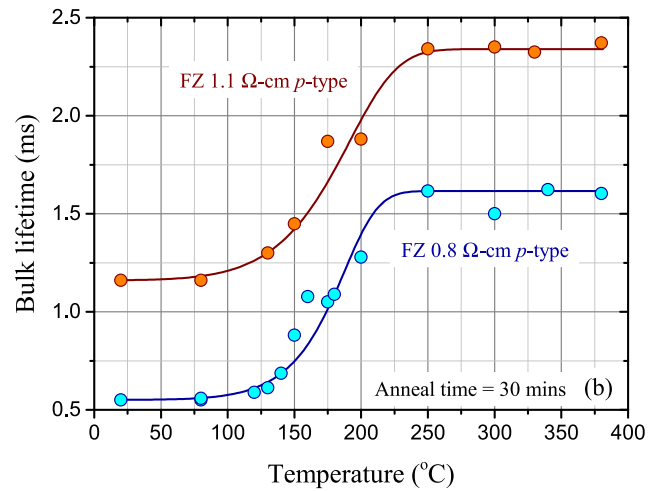
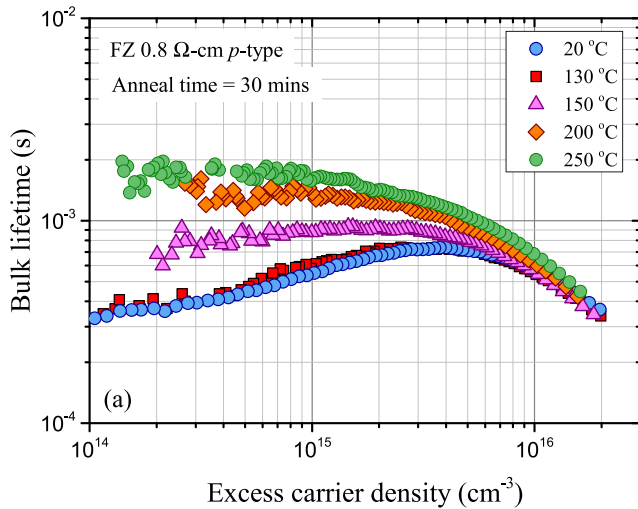


FIG. 1. (a) Injection dependent bulk lifetime for FZ 0.8  $\Omega$  cm  $p$ -type samples after annealing at 20, 130, 150, 200, and 250  $^{\circ}\text{C}$  for 30 min. (b) Bulk lifetime of FZ 0.8 (blue circles) and 1.1  $\Omega$  cm (orange circles)  $p$ -type samples at  $\Delta n = 1 \times 10^{15} \text{ cm}^{-3}$  versus annealing temperature for an annealing time of 30 min.

It must be mentioned that without a room temperature surface passivation technique, the defect shown in Figure 1 would not be observed, as dielectric films are often deposited at  $T > 200^{\circ}\text{C}$  and/or subsequently annealed at  $T = 400^{\circ}\text{C}$ . This may explain why such low temperature defects have not been reported in the literature previously in FZ silicon.

## B. Analysis on determining the annihilation energy ( $E_{\text{ann}}$ )

Figure 2 plots the remaining normalised defect concentration ( $N_t$ ) for both FZ and Cz silicon after annealing the samples for 30 min at each temperature. To determine the remaining  $N_t$  after annealing at any given temperature, the effective defect concentration was first calculated by  $N_{t,\text{initial}} = 1/\tau_{\text{activated}} - 1/\tau_{\text{deactivated}}$  and  $N_{t,\text{anneal}} = 1/\tau_{\text{anneal}} - 1/\tau_{\text{deactivated}}$ , where  $\tau_{\text{activated}}$  is the measured lifetime in the degraded state,  $\tau_{\text{anneal}}$  is referred to as the annealed lifetime, and  $\tau_{\text{deactivated}}$  is the maximum lifetime after annihilating the

defect. The remaining normalised defect density after annealing was then determined by  $N_t = N_{t,\text{anneal}}/N_{t,\text{initial}}$ . In this work, the normalised defect concentration was determined at an injection level of 10% of the net doping  $\Delta n = 0.1 \times p_0$ .

Figure 2 shows differences in both the shape and final annihilation temperature of the  $N_t(T)$  curves, i.e., for FZ silicon (red circles and green triangles), complete annihilation of the defect does not occur until a temperature of  $\sim 250^{\circ}\text{C}$  is reached. For Cz silicon (grey squares), complete annihilation occurs at a temperature of  $170^{\circ}\text{C}$ . To determine the annihilation energy of the de-activation process, we have performed a least squares fit to the data using the Arrhenius equation<sup>30</sup>

$$R_{\text{ann}}(T) = \kappa_o \exp\left(\frac{-E_{\text{ann}}}{k_b T}\right), \quad (1)$$

$$N_t(t, T) = \exp(-R_{\text{ann}}(T) \cdot t), \quad (2)$$

where  $R_{\text{ann}}$ ,  $E_{\text{ann}}$ ,  $\kappa_o$ ,  $T$ ,  $k_b$ , and  $t$  correspond to the defect annihilation rate, annihilation energy, exponential pre-factor, temperature, Boltzmann's constant, and annealing time, respectively. Both  $\kappa_o$  and  $E_{\text{ann}}$  are variables when fitting Eq. (2) to the data in Figure 2. Thus, there are multiple combinations of  $\kappa_o$  and  $E_{\text{ann}}$  that adequately fit the data in Figure 2. However, by carefully analysing the least squares fit when varying  $\kappa_o$  and  $E_{\text{ann}}$ , we obtain one combination of  $\kappa_o$  and  $E_{\text{ann}}$  which allows us to approximate the annihilation energy of the defect with the least error. To justify this analysis, we have performed a least squares fit to (i) the Cz  $p$ -type sample shown in Figure 2 and (ii) to the data presented by Schmidt *et al.*,<sup>31</sup> both of which should reveal  $E_{\text{ann}} \approx 1.3 \text{ eV}$  for the BO defect if this analysis is adequate. Figure 3 plots the results.

Figure 3 plots a least squares fit to the FZ and Cz data in Figure 3 when varying the  $\kappa_o$  and  $E_{\text{ann}}$  in Eq. (1). The solid and dashed black lines correspond to the Cz  $p$ -type sample used in this work and that of Schmidt *et al.*,<sup>31</sup> respectively. By examining the minimum in the least squares curve for the

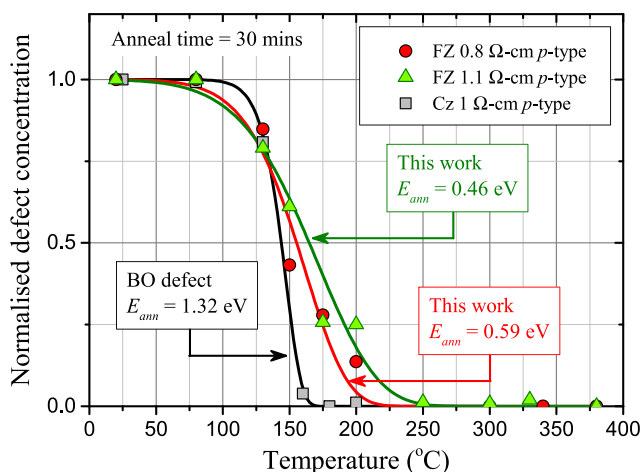


FIG. 2. (a) The remaining normalised defect concentration for FZ 0.8  $\Omega$  cm (red circles), FZ 1.1  $\Omega$  cm (green triangles), and Cz 1  $\Omega$  cm (grey squares)  $p$ -type silicon after annealing for 30 min. The green, red, and black solid lines represent best fits to the data with  $E_{\text{ann}} = 0.46$ ,  $0.59$ , and  $1.38 \text{ eV}$ , respectively.

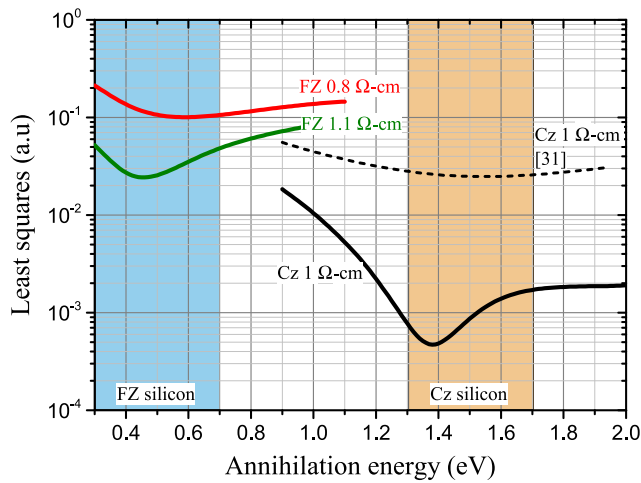


FIG. 3. Plots the least squares fit values when fitting Eq. (2) to the data in Figure 1. The red and green lines correspond to our FZ 0.8  $\Omega$  cm and 1.1  $\Omega$  cm  $p$ -type samples, while the solid and dashed black lines correspond Cz 1  $\Omega$  cm  $p$ -type samples, both from this work and from Schmidt *et al.* The blue and orange shaded areas represent the likely range of  $E_{ann}$  for each defect.

Cz sample measured in this work (solid black line), we find the minimum occurs at  $E_{ann} = 1.38$  eV, which is very close to the measured  $E_{ann}$  of 1.32 eV for the BO defect.<sup>23,30,32</sup> However, on the contrary, when the same analysis is applied to the data set of Schmidt *et al.*<sup>31</sup> (dashed black line), we find the minimum occurs at  $E_{ann} = 1.54$  eV, which is a significant deviation from the commonly measured 1.32 eV for the BO defect. The reason for this deviation is caused by the amount of scatter in the data set, evident by the much higher least squares value. Thus, while this technique can adequately predict  $E_{ann}$ , large amounts of scatter in the data set can give less certain values for  $E_{ann}$ . However, although exact values of  $E_{ann}$  may not be determined by a least squares analysis, it does allow one to specify a range of  $E_{ann}$  values, which may help to limit the number of possible defects. In the case for the two Cz samples examined in this work, we estimate that  $E_{ann}$  lies between  $1.3 < E_{ann} < 1.7$ , and thus conclude that the defect limiting the lifetime of these Cz samples is the BO defect, as expected.

Applying the same least squares analysis to the FZ data in Figure 3, we see a minimum in the least squares at  $E_{ann} = 0.46$  and 0.59 eV for the 1.1 and 0.8  $\Omega$  cm  $p$ -type samples, respectively, as shown in Figure 3. Considering these samples were sourced from the same manufacturer, it is likely that the same defect is limiting the lifetime in both samples, and thus we postulate that the slight differences in the  $E_{ann}$  values are due to the scatter in the data sets, evident by the relatively high least square values. From this analysis, we estimate that  $E_{ann}$  lies between  $0.3 < E_{ann} < 0.7$ .

### C. Experimental testing for fast diffusing metal impurities

#### 1. Phosphorus gettering of FZ $p$ -type silicon

To establish whether the defect of this work is a fast diffusing metal impurity (such as iron and copper), we have performed an impurity gettering step. Figure 4 plots the injection dependent bulk lifetime of FZ 0.8  $\Omega$  cm  $p$ -type

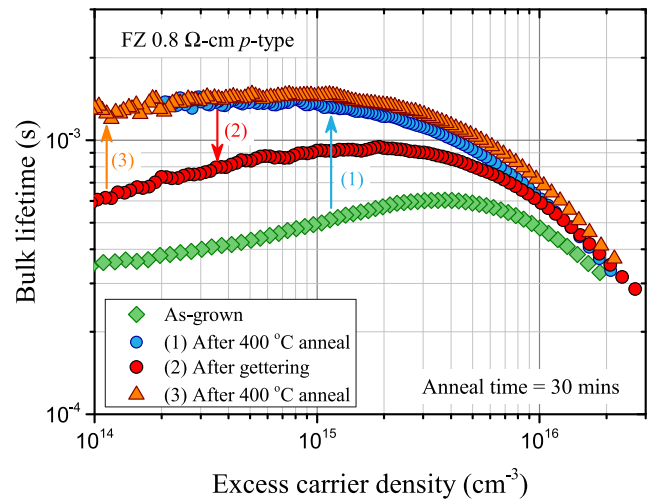


FIG. 4. Injection dependent bulk lifetime of FZ 0.8  $\Omega$  cm  $p$ -type silicon in the as-grown state (green diamonds) followed by (1) annealing at 400  $^{\circ}$ C (blue circles), (2) phosphorus gettering (red circles), and (3) subsequent annealing at 400  $^{\circ}$ C (orange triangles).

silicon in the as-grown state (green diamonds) followed by: (1) annealing at 400  $^{\circ}$ C (blue circles), (2) phosphorus gettering (red circles), and (3) subsequent annealing at 400  $^{\circ}$ C (orange triangles). The figure highlights two interesting results after phosphorus gettering. By comparing the as-grown lifetime to that after gettering, one could conclude that an improvement in  $\tau_{bulk}$  does occur, which might indicate that metal impurities were partially responsible for the low lifetimes observed for this material. However, it has already been demonstrated that low temperature annealing (250–400  $^{\circ}$ C) improves  $\tau_{bulk}$  from  $\sim 500$   $\mu$ s to  $\sim 1.5$  ms as indicated by the blue circles in Figure 4. In this case, if we compare the deactivated lifetime (blue circles) to the lifetime post gettering, it is clear that the high temperature process degrades the bulk lifetime, evident by the reduction and change in the injection dependent  $\tau_{bulk}$  curve, as represented by the red circles in Figure 4. With this additional information, we can conclude that the defect limiting the lifetime is not related to fast-diffusing metal impurities, such as iron and copper, but rather relates to point defects in the lattice (vacancies, self-interstitials) or lattice-impurity defects where the impurity is non-metallic, i.e., O, N, C, or H. To ascertain whether the defect was permanently activated after the gettering process, the 0.8  $\Omega$  cm  $p$ -type sample was subject to another 400  $^{\circ}$ C anneal for 30 min. Figure 4 demonstrates that the defect can be deactivated after a low temperature anneal, as shown by the orange triangles.

### D. Experimental testing for the boron-oxygen defect

#### 1. LID

Our results regarding the annihilation energy of the defect indicate that the observed defect is unlikely to be BO, as its annihilation energy is significantly different from the BO defect. However, to further justify this finding, we have performed LID and secondary ion mass spectroscopy (SIMS) measurements.

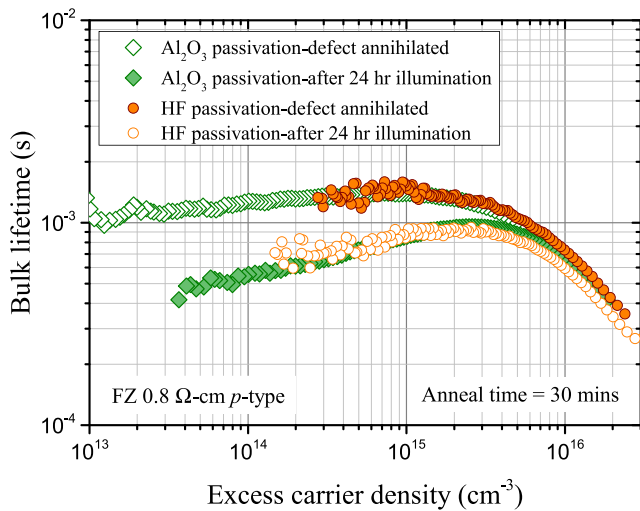


FIG. 5. Injection dependent bulk lifetime of  $\text{Al}_2\text{O}_3$  passivated  $0.8 \Omega \text{ cm}$   $p$ -type silicon before (green diamonds) and after (filled green squares)  $0.2$  sun illumination for  $24 \text{ h}$ . The figure also plots the bulk lifetime before (filled orange circles) and after (orange circles)  $0.2$  sun illumination for  $24 \text{ h}$  using HF passivation.<sup>25</sup>

Figure 5 plots the injection dependent bulk lifetime of  $\text{Al}_2\text{O}_3$  passivated  $0.8 \Omega \text{ cm}$   $p$ -type silicon before and after  $0.2$  sun illumination. Prior to the  $\text{Al}_2\text{O}_3$  deposition, the  $0.8 \Omega \text{ cm}$   $p$ -type sample was subject to a  $400^\circ\text{C}$  anneal for  $30 \text{ min}$  in a quartz tube furnace. The bulk lifetime was subsequently measured using the HF passivation method, where  $\tau_{bulk}$  of  $1.5 \text{ ms}$  was achieved (not shown). Following the room temperature  $\tau_{bulk}$  measurement, the sample was then passivated with an ALD  $\text{Al}_2\text{O}_3$  film and annealed at  $400^\circ\text{C}$  in forming gas for  $30 \text{ min}$ . The lifetime of the  $\text{Al}_2\text{O}_3$  passivated sample was measured to be  $1.4 \text{ ms}$  (open green diamonds), agreeing well with the HF passivation  $\tau_{bulk}$  measurement of  $1.5 \text{ ms}$ . The sample was then subject to  $0.2$  sun illumination for  $24 \text{ h}$  at  $\sim 60^\circ\text{C}$ , after which  $\tau_{bulk}$  was found to decrease from  $1.4 \text{ ms}$  to  $900 \mu\text{s}$  (green filled diamonds). To ascertain whether the reduction in lifetime was caused by an increase in surface or bulk recombination, the  $\text{Al}_2\text{O}_3$  film was removed in a  $10 \text{ wt. \%}$  HF solution and  $\tau_{bulk}$  was subsequently measured using the HF passivation method once again. As seen in Figure 5, the lifetime measured (orange open circles) using HF passivation exactly matches the degraded  $\text{Al}_2\text{O}_3$  passivated measurement, indicating a reduction in bulk lifetime, as shown in Figure 5. Finally, to ascertain whether the defect was permanently activated, the  $0.8 \Omega \text{ cm}$   $p$ -type sample was subject to another  $400^\circ\text{C}$  anneal for  $30 \text{ min}$ . Figure 5 demonstrates that the defect can be deactivated after a low temperature anneal, as shown by the orange filled circles, indicating that LID does not cause permanent activation.

One possible explanation for the LID observed in Figure 5 is the presence of oxygen and the recombination active BO defect.<sup>17,22,23</sup> After performing SIMS measurements, oxygen in the sample could not be detected, which indicates that the oxygen concentration is lower than the detection limit ( $2 \times 10^{16} \text{ cm}^{-3}$ ). By employing Bothe's parameterisation for the boron-oxygen-related lifetime limit, where  $[\text{O}_i] = 2 \times 10^{16} \text{ cm}^{-3}$  and  $[\text{B}] = 1.9 \times 10^{16} \text{ cm}^{-3}$ , we obtain an expected

lifetime of  $\sim 10 \text{ ms}$  after degradation,<sup>17</sup> which is too high to have an impact on the lifetime as seen in Figure 1, further suggesting that the observed defect is not related to the BO defect. However, given that Bothe's parameterisation has only been tested for  $[\text{O}_i] > 1 \times 10^{17} \text{ cm}^{-3}$ , we cannot definitively rule out the boron-oxygen defect.

Further to the results in Sec. IV C, the LID results shown in Figure 5 indicate that iron-boron pairs are not responsible for the changes in  $\tau_{bulk}$  shown in Figure 1, given that there is no cross-over point in the injection dependent lifetime curves pre and post illumination of Figure 5.<sup>33</sup>

## 2. Injection dependent lifetime spectroscopy (IDLS)

From our analysis of the annihilation energy, along with the LID and SIMS measurements, the boron-oxygen defect is an unlikely candidate for the observed defect in this work. To further strengthen this case, we analyse the recombination parameters of the defect observed here and compare it to the BO defect.

Figure 6 plots the bulk lifetime of a  $\text{FZ } 0.8 \Omega \text{ cm}$   $p$ -type silicon sample before and after annihilating the defect. The figure also plots the intrinsic (Auger and band-band radiative) lifetime limit.<sup>29</sup> From the figure, it is evident that the measured bulk lifetime of the  $0.8 \Omega \text{ cm}$   $p$ -type sample is lower than the intrinsic limit. We do not attribute this reduction in lifetime to surface recombination because the HF passivation technique used to measure the bulk lifetime reduces  $S$  to less than  $1 \text{ cm/s}$ ,<sup>27</sup> which would result in effective lifetimes of greater than  $2 \text{ ms}$  (at  $\Delta n = 1.0 \times 10^{15} \text{ cm}^{-3}$ ). Furthermore, when the same sample was passivated with ALD  $\text{Al}_2\text{O}_3$ , we attained the same lifetime post annihilation. Thus, the lower  $\tau_{bulk}$  indicates a second shallow ( $E_t - E_v < 0.1$  or  $> 1 \text{ eV}$ ) defect within the bandgap, which is limiting the bulk lifetime, as shown by the red curve in Figure 6. Unlike the dominating defect in this sample, defect 2 is not annihilated over the temperature range examined.

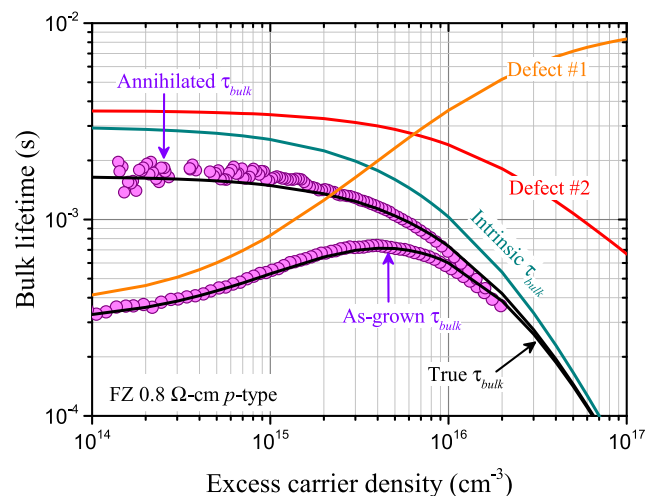


FIG. 6. Bulk lifetime of a  $\text{FZ } 0.8 \Omega \text{ cm}$   $p$ -type silicon sample before and after annihilating the defect. Also shown in the figure is the injection dependent SRH lifetime for two defects, which result when the defect is in the activated state. The figure also plots the intrinsic lifetime of Richter *et al.*<sup>29</sup>

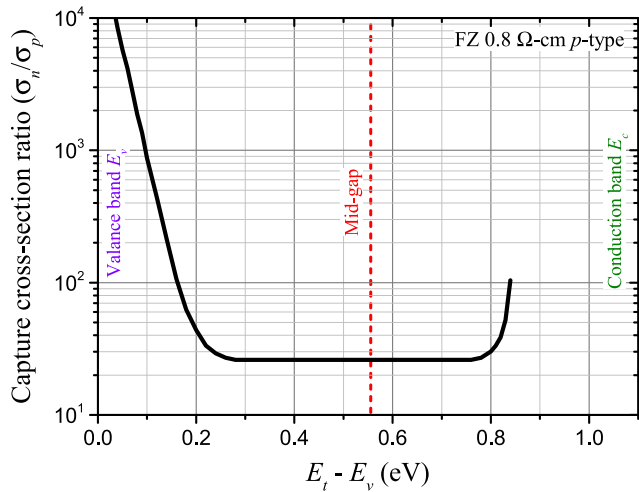


FIG. 7. Plots the capture cross section ratio ( $\sigma_n/\sigma_p$ ) of the defect as function of trap energy level above  $E_v$ .

By analysing the as-grown injection dependent  $\tau_{bulk}$  in Figure 7, information regarding the trap energy level and capture cross section ratio ( $\sigma_n/\sigma_p$ ) of the defect (#1) can be attained. We analyse these parameters using a simplified SRH method.<sup>34</sup>

Figure 7 plots the capture cross section ratio as a function of trap energy level above  $E_v$ . Although  $E_t$  and  $\sigma_n/\sigma_p$  cannot definitively be determined by this analysis, we can infer from the figure that if the defect was to have a trap energy of between 0.25–0.75 eV, then  $\sigma_n/\sigma_p \approx 26$ , suggesting that the defect is a donor level. This value is  $\sim 3$  times higher than the  $\sigma_n/\sigma_p$  ratio for the FeB and BO defects, which are commonly found in  $p$ -type silicon, providing further evidence that the defect is unlikely related to either of these metastable defects.<sup>23,33</sup>

## E. Discussion of other possible lifetime limiting defects in FZ silicon

### 1. Vacancy related defects

Vacancy concentrations in FZ silicon are predominantly determined by the growth rate of the ingot. High growth rates cause a “freeze in” of vacancies, which can remain singular; however, as vacancies are quite mobile in Si, they tend to form pairs or complexes with other vacancies or bond with impurity atoms such as P, B, C, O, N, and H.<sup>11</sup>

The most common vacancy-related defect which has been detected in c-Si by electron paramagnetic resonance is  $V_2$ ; however, in some cases V has also been detected.<sup>11,12,35–37</sup> Watkins has shown that single vacancies can be annihilated at temperatures of  $<0^\circ\text{C}$ , while divacancies require a higher annihilation temperature of  $\sim 300^\circ\text{C}$ .<sup>11</sup> Although this annihilation temperature is close to that shown in Figure 1, recent results have shown that  $E_{ann}$  for the divacancy is in the range of 1–1.3 eV,<sup>35,36,38</sup> indicating that divacancies are not the lifetime limiting defect in our samples (we estimate an  $E_{ann}$  of 0.3–0.7 eV).

If c-Si is exposed to hydrogen, whether during ingot growth or during wafer processing, H can easily diffuse into silicon, which can form vacancy-hydrogen complexes.<sup>39,40</sup>

Vacancy-hydrogen can exist in several forms, the most common being the vacancy-hydrogen (VH) and  $V_2\text{H}$  defects.<sup>11</sup> It has been suggested that VH has an energy level at  $E_c - 45$  eV and  $V_2\text{H}$  at  $E_c - 42$  eV,<sup>4,13</sup> both of which can be annihilated at temperatures of 250–300 °C.<sup>11</sup> Of the defects discussed thus far, VH and  $V_2\text{H}$  show similar low temperature annealing behaviour to the defect presented in this work. However, when the sample is annealed or processed at high temperature (880 °C), as performed in this work, it is unlikely the recombination active VH or  $V_2\text{H}$  defects reform, given that effusion of H is likely to occur at these temperatures.<sup>41</sup> Considering our samples were in the “as grown” state when the measurements shown in Figure 1 were performed, the existence of VH and  $V_2\text{H}$  implies the manufacturer grew the FZ ingot in a partial H ambient. This seems unlikely given previous studies have shown that hydrogen introduces more highly recombination active defects.<sup>9</sup> However, while VH and  $V_2\text{H}$  seem an unlikely candidate for the defect presented in this paper, evidence from the literature indicates that it is possible.

Interstitial oxygen in Cz silicon has been shown to react with silicon vacancies, forming recombination active defects such as vacancy-oxygen (VO),  $V_2\text{O}$ , and  $V_3\text{O}$ .<sup>11,39,42–44</sup> The creation of these defects in FZ silicon is also possible given that typical  $[\text{O}_i]$  concentrations are in the order of  $10^{15}\text{ cm}^{-3}$ ;<sup>19</sup> however, their concentration would be much lower in this high purity material. Recently, we uncovered the recombination activity of the vacancy-oxygen defect in Cz silicon through minority carrier lifetime spectroscopy measurements and found that the VO defect can be deactivated between 300 and 400 °C,<sup>14,45</sup> consistent with experimental and theoretical results of others.<sup>11,38,43</sup> Considering the annihilation temperature of the vacancy-oxygen defect is significantly higher than what is observed in this work, we postulate our  $p$ -type FZ material is not limited by VO defects.

The distribution of vacancies in silicon ingots is known to decrease from the centre of the wafer to the edge, where their concentration depends on the growth rate.<sup>12,46</sup> It has been shown previously that the presence of vacancy related defects can be observed using photoluminescence (PL) imaging, where they appear as circular patterns in the lifetime image.<sup>20</sup> To further investigate for the presence of vacancy-related defects, PL imaging of  $\text{Al}_2\text{O}_3$  passivated FZ 0.8 and 1.1  $\Omega\text{ cm}$   $p$ -type samples was performed. From PL imaging, the lifetime showed to be laterally uniform with no indication of circular ringlike patterns such as those resulting from vacancy and/or interstitially rich regions. However, while the PL images did not show the expected distribution of vacancies, we cannot definitively conclude that they are not related to the defect found in this work.

### 2. Carbon related defects

Carbon is the second most abundant impurity in Si (after oxygen) and commonly takes the form as a substitutional impurity ( $\text{C}_s$ ). Substitutional carbon is electrically neutral<sup>45</sup> and its concentration in FZ silicon is typically of  $10^{16}\text{ cm}^{-3}$ .<sup>18</sup> Mobile interstitial Si atoms can displace  $\text{C}_s$  from its

substitutional site, thus creating interstitial carbon ( $C_i$ ),<sup>39</sup> with energy levels at  $E_v + 0.28$  eV and  $E_c - 0.1$  eV.<sup>39,47</sup> As  $C_i$  is highly mobile at room temperature, it migrates until it reaches a stable configuration such as  $C_iC_s$  and  $C_iO_i$ .<sup>18,39,45,47</sup> The  $C_iC_s$  defect is bistable and has two energy levels within the silicon bandgap, one at  $E_v + 0.09$  eV and the other at  $E_c - 0.17$  eV.<sup>18</sup> Thus, the defect can switch between the two energy levels depending on its configuration. The  $C_iC_s$  defect, however, can only be completely annihilated after a 20 min anneal at 350 °C, substantially higher than we report in this work.<sup>18</sup> The  $C_iO_i$  configuration has one energy level at  $E_v + 0.36$  eV and is typically annihilated at 400 °C.<sup>11,39,48</sup> Asom *et al.* have shown that interstitial Si can be captured by two substitutional carbon atoms to form  $C_sSi_iC_s$ .<sup>48</sup> They showed that  $C_sSi_iC_s$  could be annihilated at temperatures of  $\sim 250$  °C and showed similar annealing characteristics to those shown in Figure 1. Thus of the defects discussed in this paper,  $C_sSi_iC_s$  is another potential candidate for the defect discovered in this work.

### 3. Nitrogen related defects

Nitrogen doping during the growth of FZ ingots has been a technique employed by silicon ingot manufacturers to improve the mechanical strength of crystals.<sup>21</sup> Little information regarding the impact of nitrogen doped silicon on the minority carrier lifetime exists; however, Cizsek *et al.* investigated the impact of nitrogen doping when the FZ ingot was grown in a  $N_2$  ambient.<sup>9,15</sup> They found in most cases  $N_2$  had little to no impact on  $\tau_{bulk}$  (where  $\tau_{bulk} \approx 4$  ms). In one case, however, N doping was found to increase  $\tau_{bulk}$  by eliminating swirl type defects. On the contrary, we have recently investigated the impact of nitrogen doping in both FZ and Cz silicon. In both cases, irrespective of the doping type ( $n$  or  $p$ ), high concentrations of nitrogen ( $> 10^{15} \text{ cm}^{-3}$ ) were found to have a substantial impact on  $\tau_{bulk}$ , where millisecond reductions in lifetime were observed.<sup>20</sup> In the case of N doped FZ silicon wafers, we found the nitrogen related defects to be significantly more recombination active in the centre of the wafers than towards the outer edge. We thus postulated the defect correlated to  $V_xN_y$  complexes, reflecting the expected distribution of vacancies.<sup>21</sup> Fortunately, the recombination activity of the  $V_xN_y$  complex can be deactivated by high temperature (1000 °C) annealing, which can increase  $\tau_{bulk}$  into the millisecond range.<sup>20,49</sup> To ascertain whether nitrogen was present in our samples, SIMS measurements were performed. From the SIMS measurements, a nitrogen concentration of  $1 \times 10^{14} \text{ cm}^{-3}$  was detected in these samples, indicating that nitrogen could form part of the recombination active defect found in this work. However, given that temperatures of 1000 °C are required to annihilate the  $V_xN_y$  defect, we suggest that vacancy-nitrogen pairs are not responsible for the reduction in  $\tau_{bulk}$  of our  $p$ -type samples as shown in Figure 1.

### 4. Composition of the defect

The work presented in this paper has uncovered a new grown-in defect limiting the lifetime of  $p$ -type FZ silicon.

TABLE I. Outlines the characteristics of the defect(s) examined in this paper.

Parameter	Defect #1 (deep level)	Defect #2 (shallow level)
$E_{ann}$ (eV)	0.3–0.7	...
$\sigma_n/\sigma_p$	$\sim 30^a$	$< 1^b$ or $> 1^c$
$E_t - E_v$ (eV)	0.25–0.75	$< 0.1$ or $> 1$
Annihilation $T$ (°C)	$250 < T < 600$	...
Activation $T$ (°C)	$> 600$	...

<sup>a</sup>If  $E_t - E_v$  lies within an energy level of 0.25–0.75 eV.

<sup>b</sup>If  $E_t - E_v$  occupies an energy level of  $< 0.1$  eV.

<sup>c</sup>If  $E_t - E_v$  occupies an energy level of  $> 1$  eV.

Table I outlines the characteristics of the defect(s) examined in this paper.

From our experimental results and those published in the literature, we postulate that the defect limiting the lifetime in our  $p$ -type samples could be a lattice-impurity or an impurity-impurity defect. Specifically, these defects could be,  $BO_{2i}$ ,  $VH$ ,  $V_2H$ ,  $C_sSi_iC_s$ , or  $N$ . While the composition of the defect remains unknown, we can conclude that the defect does not consist of a fast-diffusing metal impurity, as evidenced by the phosphorus gettering data shown in Figure 4.

## V. CONCLUSION

In this work, we have uncovered a metastable defect limiting the bulk lifetime of FZ silicon in the as-grown state using a room temperature lifetime spectroscopic technique. From a Shockley-Read-Hall analysis of the as-grown injection dependent bulk lifetime, a capture cross section ratio of  $\sim 30$  was determined, assuming  $E_t - E_v$  lies within an energy level of 0.25–0.75 eV. After annealing the FZ  $p$ -type silicon at temperatures between 80 °C and 400 °C for 30 min, the bulk lifetime was found to improve from  $\sim 500 \mu\text{s}$  to  $\sim 1.5$  ms. From our analysis of the  $N_f(T)$  curves, the activation energy for the annihilation process of the defect was determined to be  $0.3 < E_{ann} < 0.7$  eV. When the annihilated samples were phosphorus gettering at 880 °C or subject to 0.2 sun illumination for 24 h,  $\tau_{bulk}$  was found to degrade. However, when the samples were subsequently annealed at temperatures of 250–400 °C, the defect could be re-annihilated. Our results indicate that the metastable defect is not related to the BO defect or fast diffusing metal impurities such as iron and copper. Instead, from our experimental results, we postulate that the defect limiting the lifetime in our  $p$ -type FZ silicon is either a lattice-impurity or an impurity-impurity (light impurity) metastable defect.

We also note that while this work has not identified any particular defect or impurity responsible for a reduction in  $\tau_{bulk}$  in FZ silicon, it has demonstrated that caution must be taken when using FZ silicon as a control material and in surface passivation studies.

## ACKNOWLEDGMENTS

This work has been supported by the Australian Renewable Energy Agency (ARENA) fellowships program and the Australian Research Council (ARC) Future Fellowships program. Responsibility for the views, information, or advice expressed herein is not accepted by the Australian Government.

- <sup>1</sup>A. Herguth, G. Schubert, M. Kaes, and G. Hahn, *Prog. Photovoltaics* **16**, 135 (2008).
- <sup>2</sup>D. C. Walter, B. Lim, K. Bothe, V. V. Voronkov, R. Falster, and J. Schmidt, *Appl. Phys. Lett.* **104**, 042111 (2014).
- <sup>3</sup>P. Hamer, B. Hallam, S. Wenham, and M. Abbott, *IEEE J. Photovoltaics* **4**, 1252 (2014).
- <sup>4</sup>S. W. Glunz, S. Rein, J. Knobloch, W. Wettling, and T. Abe, *Prog. Photovoltaics* **7**, 463 (1999).
- <sup>5</sup>S. W. Glunz, S. Rein, J. Y. Lee, and W. Warta, *J. Appl. Phys.* **90**, 2397 (2001).
- <sup>6</sup>J. Haunschild, I. E. Reis, J. Geilker, and S. Rein, *Phys. Status Solidi RRL* **5**, 199 (2011).
- <sup>7</sup>R. Søndena, Y. Hu, M. Juel, M. S. Wiig, and H. Angelskär, *J. Cryst. Growth* **367**, 68 (2013).
- <sup>8</sup>J. D. Murphy, K. Bothe, R. Krain, V. V. Voronkov, and R. J. Falster, *J. Appl. Phys.* **111**, 113709 (2012).
- <sup>9</sup>T. F. Ciszek and T. H. Wang, in *Electrochemical Society Fall Conference*, Phoenix, Arizona (2000).
- <sup>10</sup>T. H. Wang, T. F. Ciszek, and T. Schuyler, *J. Cryst. Growth* **109**, 155–161 (1991).
- <sup>11</sup>G. D. Watkins, *Mater. Sci. Semicond. Process.* **3**, 227–235 (2000).
- <sup>12</sup>V. V. Voronkov and R. Falster, *J. Cryst. Growth* **194**, 76 (1998).
- <sup>13</sup>P. Leveque, A. Hallen, B. G. Svensson, J. Wong-Leung, C. Jagadish, and V. Privitera, *Eur. Phys. J.: Appl. Phys.* **23**, 5–9 (2003).
- <sup>14</sup>F. E. Rougieux, N. E. Grant, and D. Macdonald, *Phys. Status Solidi* **7**, 616–618 (2013).
- <sup>15</sup>T. F. Ciszek, T. H. Wang, R. W. Burrows, T. Bekkedahl, M. I. Symko, and J. D. Webb, *Sol. Energy Mater. Sol. Cells* **41/42**, 61–70 (1996).
- <sup>16</sup>P. Zheng, F. Rougieux, N. Grant, and D. Macdonald, *IEEE J. Photovoltaics* **5**, 183–188 (2015).
- <sup>17</sup>K. Bothe, R. Sinton, and J. Schmidt, *Prog. Photovoltaics* **13**, 287–296 (2005).
- <sup>18</sup>L. W. Song, X. D. Zhan, B. W. Benson, and G. D. Watkins, *Phys. Rev. B* **42**, 5765–5783 (1990).
- <sup>19</sup>M. Bruzzi, D. Menichelli, M. Scarungella, J. Harkonen, E. Tuovinen, and Z. Li, *J. Appl. Phys.* **99**, 093706 (2006).
- <sup>20</sup>F. Rougieux, N. Grant, J. Murphy, and D. Macdonald, “Influence of Annealing and Bulk Hydrogenation on Lifetime-Limiting Defects in Nitrogen-Doped Floating Zone Silicon,” *IEEE J. Photovoltaics* (to be published).
- <sup>21</sup>T. Abe, H. Harada, N. Ozawa, and K. Adomi, in *Materials Research Society Fall Meeting* (1985), Vol. 59, pp. 537–544.
- <sup>22</sup>J. Schmidt and K. Bothe, *Phys. Rev. B* **69**, 024107 (2004).
- <sup>23</sup>K. Bothe and J. Schmidt, *Appl. Phys. Lett.* **87**, 262108 (2005).
- <sup>24</sup>H. Savin, M. Yli-Koski, and A. Haarahiltunen, *Appl. Phys. Lett.* **95**, 152111 (2009).
- <sup>25</sup>N. E. Grant, K. R. McIntosh, and J. T. Tan, *ECS J. Solid State Sci. Technol.* **1**, 55 (2012).
- <sup>26</sup>R. A. Sinton and A. Cuevas, *Appl. Phys. Lett.* **69**, 2510 (1996).
- <sup>27</sup>N. E. Grant, K. R. McIntosh, J. T. Tan, F. Rougieux, J. Bullock, Y. Wan, and C. Barugkin, in *28th European Photovoltaic Solar Energy Conference*, Paris, France (2013).
- <sup>28</sup>J. Harkonen, V.-P. Lempinen, T. Juvonen, and J. Kylmälouma, *Sol. Energy Mater. Sol. Cells* **73**, 125 (2002).
- <sup>29</sup>A. Richter, S. W. Glunz, F. Werner, J. Schmidt, and A. Cuevas, *Phys. Rev. B* **86**, 165202 (2012).
- <sup>30</sup>K. Bothe and J. Schmidt, *J. Appl. Phys.* **99**, 013701 (2006).
- <sup>31</sup>J. Schmidt, A. G. Aberle, and R. Hezel, in *26th Photovoltaic Specialist Conference*, Anaheim, California (1997).
- <sup>32</sup>S. Rein, T. Rehr, W. Warta, S. W. Glunz, and G. Willeke, in *17th European Photovoltaic Solar Energy Conference*, Munich, Germany (2001).
- <sup>33</sup>D. Macdonald, A. Cuevas, and J. Wong-Leung, *J. Appl. Phys.* **89**, 7932–7939 (2001).
- <sup>34</sup>D. Macdonald and A. Cuevas, *Phys. Rev. B* **67**, 075203 (2003).
- <sup>35</sup>R. Poirier, V. Avalos, S. Dannefaer, F. Schiettekatte, and S. Roorda, *Physica B* **340–342**, 609–612 (2003).
- <sup>36</sup>P. M. Mooney, L. J. Cheng, M. Suli, J. D. Gerson, and J. W. Corbett, *Phys. Rev. B* **15**, 3836–3843 (1977).
- <sup>37</sup>A. H. Kalma and J. C. Corelli, *Phys. Rev.* **173**, 734–745 (1968).
- <sup>38</sup>P. Pellegrino, P. Leveque, J. Lalita, and A. Hallen, *Phys. Rev. B* **64**, 195211 (2001).
- <sup>39</sup>H. Malmbeek, Ph.D. dissertation, (University of Oslo, Department of Physics, 2012).
- <sup>40</sup>H. Malmbeek, L. Vines, E. V. Monakhov, and B. G. Svensson, *Phys. Status Solidi* **8**, 705–708 (2011).
- <sup>41</sup>M. Strutzmann, W. Beyer, L. Tapfer, and C. P. Herrero, *Physica B* **170**, 240–244 (1991).
- <sup>42</sup>V. Quemener, B. Raeissi, F. Herklotz, L. I. Murin, E. V. Monakhov, and B. G. Svensson, *Phys. Status Solidi B* **251**, 2197–2200 (2014).
- <sup>43</sup>V. P. Markevich, A. R. Peaker, S. B. Lastovskii, L. I. Murin, J. Coutinho, V. J. B. Torres, P. R. Briddon, L. Dobaczewski, E. V. Monakhov, and B. G. Svensson, *Phys. Rev. B* **80**, 235207 (2009).
- <sup>44</sup>J. H. Bleka, H. Malmbeek, E. V. Monakhov, and B. G. Svensson, *Phys. Rev. B* **85**, 085210 (2012).
- <sup>45</sup>H. Wang, A. Chronos, C. A. Londos, E. N. Sgourou, and U. Schwingenschlogl, *Sci. Rep.* **4**, 1–9 (2014).
- <sup>46</sup>V. V. Voronkov, *J. Cryst. Growth* **59**, 625 (1982).
- <sup>47</sup>L. W. Song and G. D. Watkins, *Phys. Rev. B* **42**, 5759–5764 (1990).
- <sup>48</sup>M. T. Asom, J. L. Benton, R. Sauer, and L. C. Kimerling, *Appl. Phys. Lett.* **51**, 256–258 (1987).
- <sup>49</sup>C. Cui, D. Yang, X. Yu, X. Ma, L. Li, and D. Que, *Microelectron. Eng.* **66**, 373–378 (2003).